Published in final edited form as:

Biomol NMR Assign. 2016 October ; 10(2): 385–389. doi:10.1007/s12104-016-9705-8.

^{1}H, ^{13}C, and ^{15}N resonance assignments and secondary structure information for *Methylobacterium extorquens* PqqD and the complex of PqqD with PqqA

Robert L. Evans III[1], **John A. Latham**[2,3], **Judith P. Klinman**[2], **Carrie M. Wilmot**[1], and **Youlin Xia**[4]

[1]Department of Biochemistry, Molecular Biology, and Biophysics, University of Minnesota, Twin Cities, Saint Paul, MN, 55108 USA

[2]Departments of Chemistry and of Molecular and Cell Biology, University of California, Berkeley, Berkeley, CA, 94720 USA

[4]Minnesota NMR Center, University of Minnesota, Twin Cities, Minneapolis, MN, 55455 USA

Abstract

The ribosomally synthesized and post-translationally modified peptide (RiPP), pyrroloquinoline quinone (PQQ), is a dehydrogenase cofactor synthesized by, but not exclusively used by, certain prokaryotes. RiPPs represent a rapidly expanding and diverse class of natural products—many of which have therapeutic potential—and the biosynthetic pathways for these are gaining attention. Five gene products from the *pqq* operon (PqqA, PqqB, PqqC, PqqD, and PqqE) are essential for PQQ biosynthesis. The substrate is the peptide PqqA, which is presented to the radical SAM enzyme PqqE by the small protein PqqD. PqqA is unstructured in solution, and only binds to PqqE when in complex with PqqD. PqqD is a member of a growing family of RiPP chaperone proteins (or domains in some cases) that present their associated peptide substrates to the initial RiPP biosynthesis enzymes. An X-ray crystal dimer structure exists for *Xanthomonas campestris* PqqD (PDB ID: 3G2B), but PqqD is now known to act as a monomer under physiological conditions. In this study, the PqqD truncation from naturally fused *Methylobacterium extorquens* (*Mex*) PqqCD was overexpressed in *Escherichia coli* and *Mex*PqqA was chemically synthesized. Solution NMR ^{1}H-,^{15}N-HSQC chemical shift studies have identified the PqqD residues involved in binding PqqA, and ^{1}H, ^{13}C, and ^{15}N peak assignments for PqqD alone and for PqqD bound to PqqA are reported herein.

Keywords

Pyrroloquinoline quinone biosynthesis; PQQ; PqqA; PqqD; NMR resonance assignments; RiPP

Corresponding author (telephone, and fax number), Carrie Wilmot, Wilmo004@umn.edu, Phone: 612-624-2406, Fax: 612-625-5780.
[3]Current address: Department of Chemistry and Biochemistry, University of Denver, Denver, CO, 80208 USA

Biological context

4,5-Dihydro-4,5-dioxo-1*H*-pyrrolo[2,3-*f*] quinolone-2,7,9-tricarboxylic acid (pyrroloquinoline quinone or PQQ), is a ribosomally synthesized and post-translationally modified peptide (RiPP) that acts as a dehydrogenase cofactor for certain alcohol and aldose sugar dehydrogenases in prokaryotes (Duine 1999; Anthony 2004). Five gene products from the *pqq* operon are required for PQQ biosynthesis (Shen et al. 2012). Two of these five products, PqqA, a 20 to 30 residue peptide with an absolutely conserved EXXXY sequence near its C-terminal end (Goosen et al. 1989; Houck et al. 1989; Unkefer et al. 1995; van Kleef and Duine 1988), and PqqD, which tightly binds PqqA and forms a ternary complex with PqqA and PqqE (Latham et al. 2015), are the focus of the NMR studies described in this paper.

PQQ is of interest for several reasons. It is a tricyclic, redox active o-quinone that is not formed by direct post-translational modification of active site residues, but instead is synthesized by way of a RiPP pathway (Goodwin 1998; Anthony 2001; Latham et al. 2015). PQQ is a significant antioxidant, and when present supports mitochondrial biogenesis and function in a wide range of organisms (Bauerly et al. 2011; Bauerly et al. 2006; Chowanadisai et al. 2010; Harris et al. 2013; Stites et al. 2006; Singh et al. 2015; Zhang et al. 2015). Additionally, PQQ demonstrates probiotic properties in mammals; studies with rats and mice have demonstrated decreased growth, reduced immune response, and declining reproductive success when subjects were deprived of PQQ in their diets (Kasahara and Kato 2003; Killgore et al. 1989; Steinberg et al. 2003; Steinberg et al. 1994). While initially considered a cofactor for prokaryotes only, a recent publication identified a fungal enzyme for which PQQ serves as cofactor (Matsumura et al. 2014). Finally, plant studies indicate that the presence of PQQ promotes growth (Okhee et al. 2008).

Only one structural model of PqqD has been published, and this is a dimeric crystal structure of *Xanthomonas campestris* (*Xc*) PqqD (PDB ID: 3G2B). However, the physiological state of PqqD is monomeric (Latham et al., 2015), so the biological relevance of the *Xc*PqqD structure is uncertain. In this study, the PqqD portion of the natural *Methylobacterium extorquens* (*Mex*) fusion PqqCD was expressed in *Escherichia coli* to give ^{13}C and ^{15}N isotopically labeled protein, which was purified and subjected to NMR spectroscopic analysis. The interaction of the isotopically labeled *Mex*PqqD with unlabeled and chemically synthesized *Mex*PqqA, which binds with a K_d of ~ 200 nM (Latham et al. 2015), was also probed by NMR spectroscopy. Here we present the *Mex*PqqD resonance and secondary structure assignments in the absence and presence of *Mex*PqqA in the pursuit of the physiological structure of PqqD and the mapping of the interaction surface of PqqA on PqqD.

Methods and experiments

Recombinant protein expression and purification

Materials—The T4 DNA ligase and restriction enzymes were obtained from New England BioLabs (Ipswich, MA). Polymerase was obtained from Agilent Technologies (Santa Clara,

CA). Oligonucleotides were obtained from Eurofins (Huntsville, AL). All DNA sequencing was performed by the University of California's DNA Sequencing Facility (Berkeley, CA).

Preparation of PqqA—The unlabeled peptide, *Mex*PqqA ΔM1, C12S (derived from the wild type, UniProt # Q49148), was synthesized and purified to >80% purity by CPC Scientific (Emeryville, CA) and then used at that purity. The peptide sequence, KWAAPIVSEISVGMEVTSYESAEIDTFN, incorporated a serine in place of the cysteine at residue position 11 to eliminate spurious dimer formation.

Preparation of ^{15}N- and ^{13}C-labeled, recombinant PqqD—The *MexpqqD* gene (corresponding to amino acids 280-372 from the natural *Mex*PqqCD fusion) was cloned into the pET28a vector (EMD Millipore) using the *NdeI* and *XhoI* restriction sites. The cloned gene, incorporating an N-terminal His_6-tag, was sequence verified and used to transform *E. coli* BL21 (DE3) for gene expression. Transformed *E. coli* BL21 (DE3) cells were grown aerobically at 37°C in M9 minimal media supplemented with 1 g/L NH_4Cl (99% ^{15}N, Cambridge Isotopes, Tewksbury, MA), 4 g/L D-glucose (U-^{13}C, Cambridge Isotope Laboratories, Tewksbury, MA) and 50 μg/mL kanamycin. Cells were induced with 1 mM IPTG when the OD_{600} reached 0.6. Following a 12 h induction at 20°C, the cells were harvested by centrifugation at 6,500 rpm for 10 min. The cells were suspended in five times the mass of cell paste of 50 mM PBS (pH 7.5) and 50 mM imidazole. The cells were lysed by sonication, and the lysate was centrifuged at 20,000 rpm for 15 min. The supernatant was loaded onto a 5 mL HisTrap FF column (GE Healthcare) and the column was washed at 4°C with lysis buffer to remove non-tagged protein, and then with 50 mM PBS (pH 6.5) and 300 mM imidazole to elute the tagged protein. The desired fractions were combined, concentrated, and buffer exchanged over PD-10 columns (GE Healthcare) equilibrated with 25 mM phosphate buffer (pH 6.5). Yield for His_6-tagged ^{13}C-,^{15}N-labeled *Mex*PqqD: 27 mg/L culture.

Experimental quantities—NMR experiments were performed using D_2O matched Shigemi microtubes, 5 mm O.D. (Shigemi, Inc.). The experimental solution for PqqD alone contained 285 μL of 5.0 mg/ml (0.40 mM) ^{13}C-,^{15}N-labeled *Mex*PqqD in 25 mM potassium phosphate, pH 6.5, 7 μL of 50 mM sodium azide, and 15 μL HPLC grade D_2O (final concentrations: 4.6 mg/ml (0.37 mM) *Mex*PqqD, 1.1 mM sodium azide, 4.9% D_2O).

The experimental solution for PqqD bound to PqqA (in approximately 4-fold molar excess) was identical to the PqqD alone with the inclusion of 1.35 mg lyophilized, unlabeled *Mex*PqqA (final concentrations: 4.6 mg/ml (0.37 mM) *Mex*PqqD, 4.4 mg/ml *Mex*PqqA (1.4 mM), 1.1 mM sodium azide, 4.9% D_2O).

NMR spectroscopy

All NMR data were recorded at 25°C on Bruker AVANCE™ III 850 or 900 MHz NMR spectrometers, each with 5 mm TCI CryoProbes including shielded z-gradient. Two sets of NMR data were acquired with the two samples, ^{13}C-,^{15}N-labeled PqqD and ^{13}C-,^{15}N-labeled PqqD + unlabeled PqqA. The tight binding of PqqD and PqqA precluded a titration approach. Data were processed with nmrPipe (Delaglio, et al. 1995). Proton chemical shifts

were calibrated with respect to the water signal relative to DSS ($(CH_3)_3Si(CH_2)_3SO_3Na$); ^{15}N and ^{13}C chemical shifts were indirectly referenced to DSS (Live, et al. 1984). Linear predictions were applied to the ^{15}N and ^{13}C dimensions to double the data size and improve digital resolution. A cosine square window function and “auto” zero filling were applied to all ^{1}H, ^{15}N and ^{13}C dimensions. Data were analyzed with Sparky (Goddard and Kneller).

Experiments—Sequence-specific backbone assignments were completed using AutoAssign with two 3D spectra: HNCACB and CBCA(CO)NH (Zimmerman, et al. 1997; Muhandiram, et al. 1994). The HNCACB creates both intra- and inter-residue correlations, whereas the CBCA(CO)NH creates only inter-residue correlations. Combining these two spectra, backbone chemical shifts, including $^{1}H_N$, ^{15}N, ^{13}CA, ^{13}CB, were assigned. $^{13}C'$ chemical shifts were assigned using a 3D HNCO and the first 2D ^{1}H-^{13}C plane of 3D HNCACO (Kay, et al. 1994). ^{1}H and ^{13}C side chain assignments were performed with HCCH-TOCSY, H(CCCO)NH and C(CCO)NH (mixing time: 16 ms) (Montelione, et al. 1992; Kay, et al. 1993). HA assignments and scalar J coupling $^{3}J_{HNHA}$ were obtained from 3D HNHA spectrum (Vuister and Bax, 1994). The $^{1}H_{\delta}$ and $^{1}H_{e}$ resonances of aromatic residues were assigned using 2D (HB)CB(CGCD)HD and (HB)CB(CGCDCE)HE (Yamazaki, et al. 1993).

Results

Backbone and sidechain ^{1}H, ^{15}N, and ^{13}C chemical shifts were assigned at 100% with the exception of 14 of 27 aromatic ^{13}C's (52%) and 4 of 21aromatic ^{1}H's (19%), which were not assigned. A superposition of the 2D ^{1}H-^{15}N HSQC spectra for PqqD (blue peaks) and PqqD + PqqA (red peaks) is shown in Figure 1. From this plot, changes in the chemical shifts of ^{1}H and ^{15}N can clearly be identified.

Secondary structure information

The chemical shifts of $^{1}H_{\alpha}$, $^{13}C_{\alpha}$, $^{13}C_{\beta}$ and ^{13}CO resonances were used as an input to TALOS+ and CSI2.0 to predict the secondary structures of the two samples (Shen, et al. 2009; Wishart and Sykes, 1994). As shown in Figure 2, the secondary structures predicted from the two methods for PqqD in each sample are very similar. The main difference observed between the two samples, PqqD and PqqD + PqqA, is that one β-strand from the sequence fragment RTFDL of PqqD is significantly longer in the presence of PqqA. In addition, the order parameters predicted by TALOS+ and the flexibility predicted by CSI2.0 are consistent between each sample. Besides the N-terminus of PqqD (residues 1 and 8), the region between residues 51 and 56 in both samples indicates high mobility and disorder.

Assignments and data deposition

The complete backbone and side chain chemical shift assignments have been deposited in the BioMagResBank database (www.bmrb.wisc.edu) with accession numbers 26634 and 26690 for samples PqqD and PqqD + PqqA, respectively.

Acknowledgments

Financial support for this work came from the National Institutes of Health grants GM-066569 (CMW) and GM-039296 (JPK). Special thanks to the Minnesota NMR Center for both professional expertise and access to spectrometers, and to the Minnesota Supercomputing Institute for their assistance in installing and configuring the annealing software to run on *Mesabi* (reducing 20 hour anneals to 30 minutes).

References

Anthony C. Pyrroloquinoline quinone (PQQ) and quinoprotein enzymes. Antioxidant Redox Signal. 2001; 3:757–774.

Anthony C. The quinoprotein dehydrogenases for methanol and glucose. Arch Biochem Biophys. 2004; 428(1):2–9. [PubMed: 15234264]

Bauerly K, Harris C, Chowanadisai W, Graham J, Havel PJ, Tchaparian E, Satre M, Karliner JS, Rucker RB. Altering pyrroloquinoline quinone nutritional status modulates mitochondrial, lipid, and energy metabolism in rats. PLoS One. 2011; 6(7):e21779. [PubMed: 21814553]

Bauerly KA, Storms DH, Harris CB, Hajizadeh S, Sun MY, Cheung CP, Satre MA, Fascetti AJ, Tchaparian E, Rucker RB. Pyrroloquinoline quinone nutritional status alters lysine metabolism and modulates mitochondrial DNA content in the mouse and rat. Biochim Biophys Acta. 2006; 1760(11):1741–8. [PubMed: 17029795]

Choi O, Kim J, Kim JG, Jeong Y, Moon JS, Park CS, Hwang I. Pyrroloquinoline quinone is a plant growth promotion factor produced by *Pseudomonas fluorescens* B16. Plant Physiology. 2008; 146:657–668. [PubMed: 18055583]

Chowanadisai W, Bauerly KA, Tchaparian E, Wong A, Cortopassi GA, Rucker RB. Pyrroloquinoline quinone stimulates mitochondrial biogenesis through cAMP response element-binding protein phosphorylation and increased PGC-1alpha expression. J Biol Chem. 2010; 285(1):142–52. [PubMed: 19861415]

Delaglio F, Grzesiek S, Vuister GW, Zhu G, Pfeifer J, Bax A. NMRPipe: a multidimensional spectral processing system based on UNIX pipes. J Biomol NMR. 1995; 6:277–293. [PubMed: 8520220]

Duine JA. The PQQ story. J Biosci Bioeng. 1999; 88(3):231–6. [PubMed: 16232604]

Goddard, TD.; Kneller, DG. SPARKY 3. University of California; San Francisco:

Goodwin PM, Anthony C. The biochemistry, physiology and genetics of PQQ and PQQ-containing enzymes. Adv Microb Physiol. 1998; 40:1–80. [PubMed: 9889976]

Goosen N, Horsman HP, Huinen RG, van de Putte P. *Acinetobacter calcoaceticus* genes involved in biosynthesis of the coenzyme pyrrolo-quinoline-quinone: nucleotide sequence and expression in *Escherichia coli* K-12. J Bacteriol. 1989; 171(1):447–55. [PubMed: 2536663]

Harris CB, Chowanadisai W, Mishchuk DO, Satre MA, Slupsky CM, Rucker RB. Dietary pyrroloquinoline quinone (PQQ) alters indicators of inflammation and mitochondrial-related metabolism in human subjects. J Nutr Biochem. 2013; 24(12):2076–84. [PubMed: 24231099]

Houck DR, Hanners JL, Unkefer CJ, van Kleef MA, Duine JA. PQQ: biosynthetic studies in *Methylobacterium* AM1 and *Hyphomicrobium* X using specific ^{13}C labeling and NMR. Antonie Van Leeuwenhoek. 1989; 56(1):93–101. [PubMed: 2549867]

Kasahara T, Kato T. Nutritional biochemistry: A new redox-cofactor vitamin for mammals. Nature. 2003; 422(6934):832. [PubMed: 12712191]

Kay LE, Xu GY, Yamazaki T. Enhanced-sensitivity triple-resonance spectroscopy with minimal H_2O saturation. J Magn Reson. 1994; A109:129–133.

Kay LE, Xu GY, Singer AU, Muhandiram DR, Forman-Kay JD. A gradient-enhanced HCCH-TOCSY experiment for recording side-chain ^{1}H and ^{13}C correlations in H_2O samples of proteins. J Magn Reson. 1993; B101:333–337.

Killgore J, Smidt C, Duich L, Romero-Chapman N, Tinker D, Reiser K, Melko M, Hyde D, Rucker RB. Nutritional importance of pyrroloquinoline quinone. Science. 1989; 245(4920):850–2. [PubMed: 2549636]

Latham JA, Iavarone AT, Barr I, Juthani PV, Klinman JP. PqqD is a novel peptide chaperone that forms a ternary complex with the radical S-adenosylmethionine protein PqqE in the pyrroloquinoline quinone biosynthetic pathway. J Biol Chem. 2015; 290(20):12908–18. [PubMed: 25817994]

Live DH, Davis DG, Agosta WC, Cowburn D. Long Range Hydrogen Bond Mediated Effects in Peptides: 15N NMR Study of Gramicidin S in Water and Organic Solvents. J Am Chem Soc. 1984; 106:1939–1941.

Matsumura H, Umezawa K, Takeda K, Sugimoto N, Ishida T, Samejima M, Ohno H, Yoshida M, Igarashi K, Nakamura N. Discovery of a eukaryotic pyrroloquinoline quinone-dependent oxidoreductase belonging to a new auxiliary activity family in the database of carbohydrate-active enzymes. PLoS One. 2014; 9(8):e104851. [PubMed: 25121592]

Montelione GT, Lyons BA, Emerson SD, Tashiro M. An efficient triple resonance experiment using carbon-13 isotropic mixing for determining sequence-specific resonance assignments of isotopically-enriched proteins. J Am Chem Soc. 1992; 114:10974–75.

Muhandiram DR, Kay LE. Gradient-enhanced triple-resonance three-dimensional experiments with improved sensitivity. J Magn Reson. 1994; B103:203–216.

Shen Y, Delaglio F, Cornilescu G, Bax A. TALOS+: A hybrid method for predicting protein backbone torsion angles from NMR chemical shifts. J Biomol NMR. 2009; 44:213–22. [PubMed: 19548092]

Shen YQ, Bonnot F, Imsand EM, RoseFigura JM, Sjolander K, Klinman JP. Distribution and properties of the genes encoding the biosynthesis of the bacterial cofactor, pyrroloquinoline quinone. Biochemistry. 2012; 51(11):2265–75. [PubMed: 22324760]

Singh AK, Pandey SK, Saha G, Gattupalli NK. Pyrroloquinoline quinone (PQQ) producing *Escherichia coli* Nissle 1917 (EcN) alleviates age associated oxidative stress and hyperlipidemia, and improves mitochondrial function in ageing rats. Exp Gerontol. 2015; 66:1–9. [PubMed: 25843018]

Steinberg F, Stites TE, Anderson P, Storms D, Chan I, Eghbali S, Rucker R. Pyrroloquinoline quinone improves growth and reproductive performance in mice fed chemically defined diets. Exp Biol Med. 2003; 228(2):160–6.

Steinberg FM, Gershwin ME, Rucker RB. Dietary pyrroloquinoline quinone: growth and immune response in BALB/c mice. J Nutr. 1994; 124(5):744–53. [PubMed: 8169668]

Stites T, Storms D, Bauerly K, Mah J, Harris C, Fascetti A, Rogers Q, Tchaparian E, Satre M, Rucker RB. Pyrroloquinoline quinone modulates mitochondrial quantity and function in mice. J Nutr. 2006; 136(2):390–6. [PubMed: 16424117]

Unkefer CJ, Houck DR, Britt BM, Sosnick TR, Hanners JL. Biogenesis of pyrroloquinoline quinone from ^{13}C-labeled tyrosine. Methods Enzymol. 1995; 258:227–35. [PubMed: 8524153]

van Kleef MA, Duine JA. L-tyrosine is the precursor of PQQ biosynthesis in *Hyphomicrobium* X. FEBS Lett. 1988; 237(1-2):91–7. [PubMed: 2844590]

Vuister GW, Bax A. Measurement of four-bond H^N-H^α J-couplings in staphylococcal nuclease. J Biomol NMR. 1994; 4:193–200. [PubMed: 8019134]

Wishart DS, Sykes BD. The ^{13}C Chemical-Shift Index: A simple method for the identification of protein secondary structure using ^{13}C chemical-shift data. J Biomol NMR. 1994; 4:171–180. [PubMed: 8019132]

Yamazaki T, Forman-Ka JD, Kay LE. Two-dimensional NMR experiments for correlating $^{13}C_\beta$. and $^1H_{\delta/e}$ chemical shifts of aromatic residues in ^{13}C-labeled proteins via scalar couplings. J Am Chem Soc. 1993; 115:11054–11055.

Zhang J, Meruvu S, Bedi YS, Chau J, Arguelles A, Rucker R, Choudhury M. Pyrroloquinoline quinone increases the expression and activity of Sirt1 and -3 genes in HepG2 cells. Nutr Res. 2015; 35(9):844–9. [PubMed: 26275361]

Zimmerman DE, Kulikowski CA, Huang Y, Feng W, Tashiro M, Shimotakahar S, Chien C, Power R, Montelione GT. Automated analysis of protein NMR assignments using methods from artificial intelligence. J Mol Biol. 1997; 269:592–610. [PubMed: 9217263]

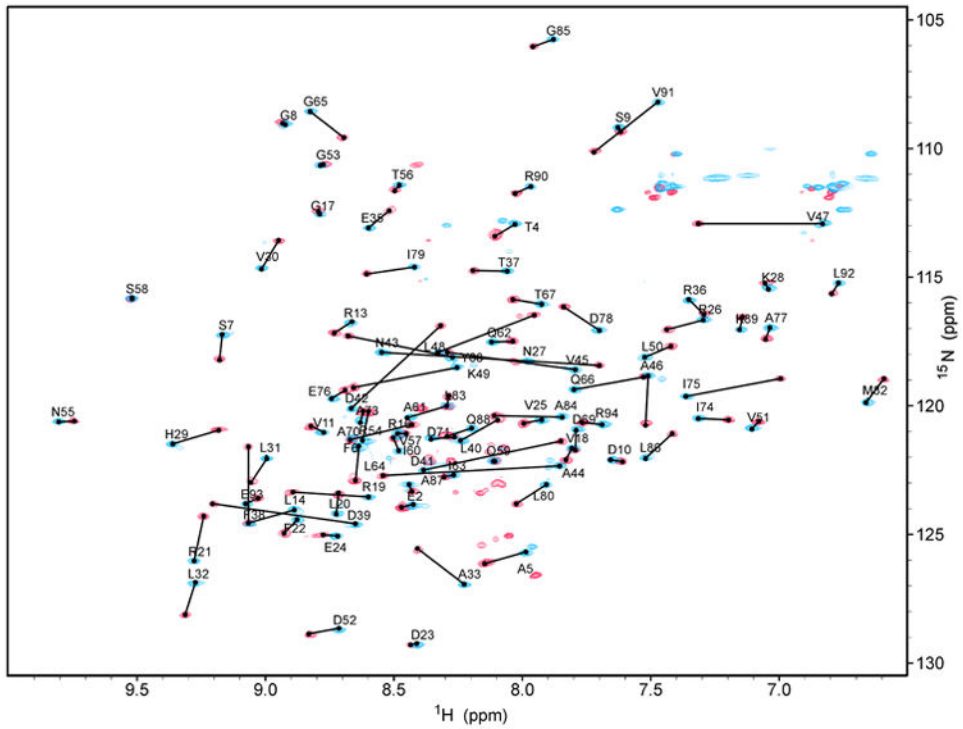

Figure 1.

Overlay of 2D ^{1}H-^{15}N HSQC spectra for ^{13}C-,^{15}N-labeled *Mex*PqqD (blue) and ^{13}C-,^{15}N-labeled *Mex*PqqD + unlabeled *Mex*PqqA (red) showing peak shifts.

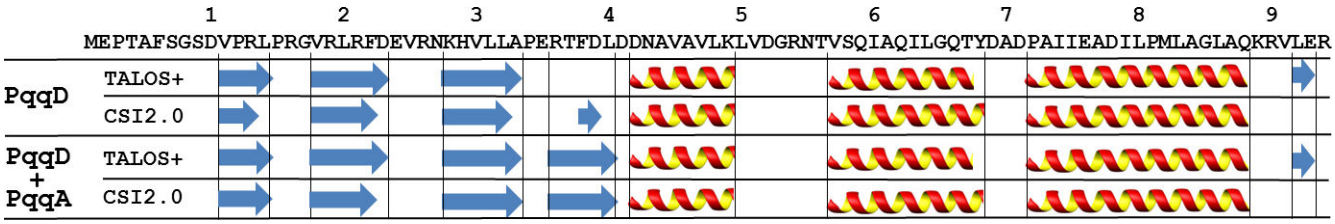

Figure 2.

Secondary structures predicted by TALOS+ and CSI2.0 for *Mex*PqqD (the first two rows) and *Mex*PqqD + *Mex*PqqA (the last two rows). The *Mex*PqqD sequence is shown above the secondary structure predictions with sequence decades indicated. Arrows and helices represent β-strand and α-helix, respectively.